ChemPhotoChem

Research Article
doi.org/10.1002/cptc.202400022

Chemistry Europe
European Chemical Societies Publishing

www.chemphotochem.org

Covalent and Visible-Light Photoswitchable Derivatives of the Potent Synthetic Opioid Isotonitazene and Other Nitazenes

Ranit Lahmy,[a] Harald Hübner,[b] Peter Gmeiner,*[b] and Burkhard König*[a]

Isotonitazene belongs to a potent class of μ-opioid receptor (μOR) ligands, known as nitazenes. The lack of knowledge surrounding this agonist and others in its class has sparked thorough re-investigations. To aid in these investigations, the purportedly covalent yet underexplored nitazene BIT was biochemically re-evaluated in this work, along with a newly synthesized analogue, Iso-BIT. Moreover, in the pursuit of understanding the mechanism, function and interactions of the μOR, this study involved developing photoswitchable nitazene derivatives as potential probe molecules. Converting known ligands into azo-containing photoswitchable derivatives offers the opportunity to modulate ligand structure with light, allowing for photocontrol of compound activity. While photocontrol of μOR activity could not be entirely achieved, photophysical evaluation of these 2-benzimidazole azo-arenes revealed a novel photoswitch scaffold that responds to visible light. Furthermore, azo-containing **2e** and **3e** emerged as promising nitazene derivatives that were able to form an exceptionally high fraction of covalent-ligand receptor complexes with wild-type μOR at physiological pH.

Introduction

Isotonitazene has been coined a 'life-threatening' substance that belongs to an emerging class of synthetic opioids, known as nitazenes.[1] This potent agonist that targets the μ-opioid receptor (μOR), a G-protein-coupled receptor (GPCR), has sparked great concern since its detection in 2019 across illicit drug markets in Europe, Canada and the United States.[1–2] Despite being first characterized in 1960 with a potency 500-fold greater than morphine,[3] isotonitazene did not become a regulated drug in these regions until its recent detection and its subsequent association with several fatal overdoses.[1b,4] Interestingly, isotonitazene was amongst several other potent 2-benzylbenzimidazole derivatives (nitazenes) that were investigated in the 1950s and 1960s as potential analgesics.[3,5] Even though these derivatives did not become clinically approved as medication, several analogues became officially regulated during this period.[2b,6] This includes a less potent structural analogue of isotonitazene, clonitazene, and a more potent analogue, etonitazene, with the latter reported at the time to be 1000-fold more potent than morphine.[3–4]

When compared to complex poppy alkaloids, synthetic nitazene opioids possess a simpler structure, making them easier to produce. This ease may account for their increase in popularity and could become dangerous when considering the plethora of unregulated nitazene derivatives that could be produced in the future. As a result, the stark re-emergence of isotonitazene triggered concerns about the lack of knowledge associated with this compound and its derivatives.[4,7]

While numerous nitazenes, including isotonitazene, have very recently been re-investigated and reviewed,[2,4,7–8] other derivatives require further attention. This includes the purportedly irreversible μOR agonist that was first documented in 1983, BIT (reported as 2-(*p*-ethoxy-benzyl)-1-diethylaminoethyl-5-isothiocyanobenzimidazole isothiocyanate).[9] The structure of BIT was modeled on the potent ligand etonitazene and contains a reactive isothiocyanate (NCS) in place of the 5-nitro group (Figure 1). The NCS moiety displays reactivity toward both sulfhydryl and amine nucleophiles, showcasing resistance to hydrolysis mediated by water and alcohol. This makes them well-suited candidates for covalent conjugation.[10] Although the precise μOR residue forming a covalent bond with the isothiocyanate in BIT remains unknown, BIT served as a recognized μOR alkylating agent in the 1980s, 1990s and early 2000s.[11] However, over the past two decades, BIT seems to have completely fallen out of discussion, potentially due to the emergence of more popularized opioid alternatives. It should be noted that an azido etonitazene derivative was developed in 1990 as an effective photoactivatable μOR alkylating agent, however, received even less attention.[12] This is particularly noteworthy as a covalent nitazene-based ligand, selectively targeting the μOR, could be of value in understanding nitazene

[a] *Dr. R. Lahmy, Prof. Dr. B. König*
Institute of Organic Chemistry
Department of Chemistry and Pharmacy
University of Regensburg
93053 Regensburg (Germany)
E-mail: burkhard.koenig@chemie.uni-regensburg.de

[b] *Dr. H. Hübner, Prof. Dr. P. Gmeiner*
Department of Chemistry and Pharmacy
Friedrich-Alexander University
91058 Erlangen (Germany)
E-mail: peter.gmeiner@fau.de

Supporting information for this article is available on the WWW under https://doi.org/10.1002/cptc.202400022

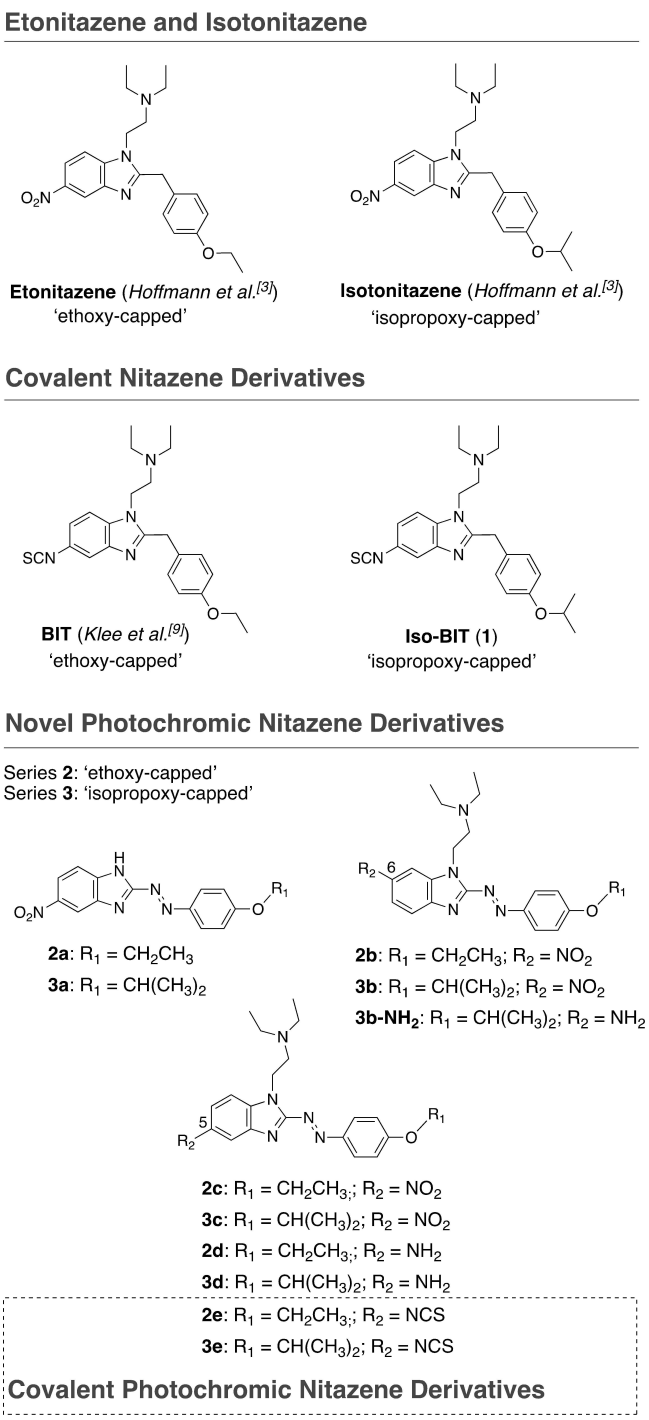

Figure 1. Structures of nitazenes explored in this work that target the μOR. This includes the model compounds etonitazene and isotonitazene, along with their isothiocyanate-containing derivatives BIT and the newly designed Iso-BIT (**1**), respectively. The photochromic derivatives, modeled on etonitazene (series 2) and isotonitazene (series 3), possess a 2-benzimidazole azoarene moiety within their core.

interactions with the μOR. Improved knowledge of this complex GPCR is crucial, particularly for the development of physiologically-biased opioids capable of inducing desirable analgesic responses while avoiding harmful side effects.[13] Although theoretical and computational research has provided insights into the protein-ligand interactions of μOR and nitazenes,[8e,14] a covalent ligand may provide access to further powerful technologies for clarifying these interactions, such as ligand-bound protein crystallography. Given that protein crystallography has played a crucial role in elucidating the function and interactions of the μOR,[15] employing this technique could enhance our understanding of the remarkable potencies of nitazene ligands.

In this work, we re-evaluated the covalent binding properties of BIT to the μOR and investigated the biological properties of a newly synthesized NCS-containing derivative that was modeled on the structure of isotonitazene, referred to here as Iso-BIT (**1**, Figure 1). In addition to such covalent probes, photochromic probes modeled on both etonitazene and isotonitazene were developed to contain a photoswitchable azo functionality within their core. This series also included reactive NCS-containing derivatives to achieve both covalent and photoswitchable systems (Figure 1). In comparison to freely diffusible analogues, covalent photoswitchable ligands targeting endogenous receptors offer improved site-selectivity and resistance to sample washing while minimizing off-target interactions.[16] Broadly speaking, the primary advantage of photoswitchable ligands lies in their ability to function as tools for spatially and temporally controlling ligand activity with light. They are extensively explored in the field of photopharmacology,[17] and have already proven beneficial in elucidating the mechanisms and interactions of the μOR, alongside other photoresponsive molecules.[18] Moreover, photophysical analysis of the photochromic series described in this work provides insights into a novel benzimidazole-based photoswitchable scaffold that responds to visible light.

Overall, this research describes the synthesis and photophysical evaluations of novel photochromic nitazenes, as well as the synthesis of nitazene derivatives containing an isothiocyanate functionality for covalent linkage to the μOR. The potency and covalent binding properties of these synthetic opioids toward the μOR were assessed through *in-vitro* biochemical assays to gain insights into their interaction with the μOR and provide valuable data for potential applications in drug development.

Results and Discussion

The most explored photoswitchable units in photopharmacology are the azobenzenes, which can either be linked to or incorporated into the structure of a bioactive molecule.[19] Upon exposure to light of a specific wavelength, azobenzenes undergo reversible isomerization, producing *cis*- or *trans*-isomeric states. The *cis*-isomer typically reverts back to the more stable *trans*-isomer thermally or upon exposure to light of a different wavelength.[19] The geometrical distinctions between *cis*- and *trans*-isomers may lead to differences in receptor binding, resulting in compounds that can exist in either a biologically active or inactive state. Such photoswitchable probes have been previously reported in the GPCR field.[20]

In recent years, research in this field has expanded beyond azobenzenes and into a variety of arylazoheterocycles. The replacement of one or both benzene units with various heterocycles has introduced diverse photophysical properties, including red-shifted absorbances and quantitative photoisomerization, which can be tuned with minor chemical modifications.[21] Additionally, arylazoheterocycles are scaffolds found in many medically-relevant biomolecules exhibiting anti-cancer, anti-inflammatory and anti-microbial properties,[22] prompting a desire to investigate how these scaffolds within such compelling molecules respond to light stimuli.

Turning the focus back to nitazenes, synthetic incorporation of the azo group into the core of etonitazene, isotonitazene, BIT and Iso-BIT resulted in the formation of benzimidazole-based arylazoheterocycles with various substitution patterns (Figure 1). Similar to other heterocycles, benzimidazoles have been reported as important scaffolds in various medicinal applications.[23] While studies have been performed to describe the photophysical nature of arylazobenzimidazoles and similar structures,[24] little was known about these properties when the aryl azo group is directly installed at position 2 of the benzimidazole unit. However, in the course of preparing this manuscript, *Decker et al.* successfully reported novel photophysical characterizations of such 2-benzimidazole azo-arenes.[25] These newly reported derivatives, designed as cannabinoid type 2 receptor agonists, differ in substitution patterns and photophysical properties from those explored in this work, exemplifying the sensitivity of this class of photoswitchable scaffolds to minor chemical modification.

While BIT was commercially available, we report herein the structure and synthesis of Iso-BIT (**1**) for the first time. To obtain Iso-BIT (**1**), the precursor isotonitazene was synthesized according to established procedures.[4] Subsequently, the nitro group of isotonitazene was reduced to amine **4** using H_2 and Pd/C (Figure 2A). Amine **4** was directly subjected to a reported NCS-forming reaction,[26] resulting in Iso-BIT with an overall yield of 29%.

The synthesis of the photochromic etonitazene series **2** began with the commercially available 5-nitro-1*H*-benzimidazol-2-ylamine (**5**, Figure 2B). To form the 2-benzimidazole azo-arene unit, an oxidative method was employed[27] with N-chlorosuccinimide as a mild oxidant, 1,8-diazabicyclo[5.4.0]undec-7-ene (DBU) in catalytic amounts and 4-ethoxyaniline, obtaining **2a** in 13% yield. This intermediate was then alkylated, using 2-chloro-*N*,*N*-diethylethylamine hydrochloride, where tautomerization resulted in regioisomers **2b** (6-nitro) and **2c** (5-nitro) with 22% and 16% yield, respectively. Given that the nitro group at position 5 is characteristic of etonitazene, we further reduced the nitro unit of **2c** to amine **2d** in 52% yield using H_2 and Pd/C. A one-pot synthesis procedure allowed the conversion of amine **2d** to isothiocyanate **2e** in 49% yield.[26]

For the photochromic isopropoxy series **3**, the same procedures were employed (Figure 2B). The azo unit was installed onto the commercially available precursor **5** using N-chlorosuccinimide, DBU and 4-isopropoxyaniline to obtain **3a** in 8% yield. Subsequent alkylation with 2-chloro-*N*,*N*-diethylethylamine hydrochloride afforded regioisomers **3b** and **3c** in 26% and 23% yield, respectively. X-ray crystal structures of these isomers were obtained, which validated their molecular structure and configuration (Figure 3). Reduction of the nitro group of both isomers (separately) resulted in amine **3b-NH$_2$** and **3d** in 8% and 33% yield, respectively. The lower yield of **3b-NH$_2$** was found to result from cleavage of the azo group under the respective reaction conditions. A one-pot synthesis allowed the conversion of amine **3d** to the isothiocyanate **3e** in 48% yield.

The photophysical evaluations of the 2-benzimidazole azo-arenes involved obtaining UV/Vis absorption spectra at thermal equilibrium and spectra of the respective *trans*- and *cis*-isomers. Additionally, evaluations included assessing cycle performances and photostationary states (PSS), as well as determining thermal

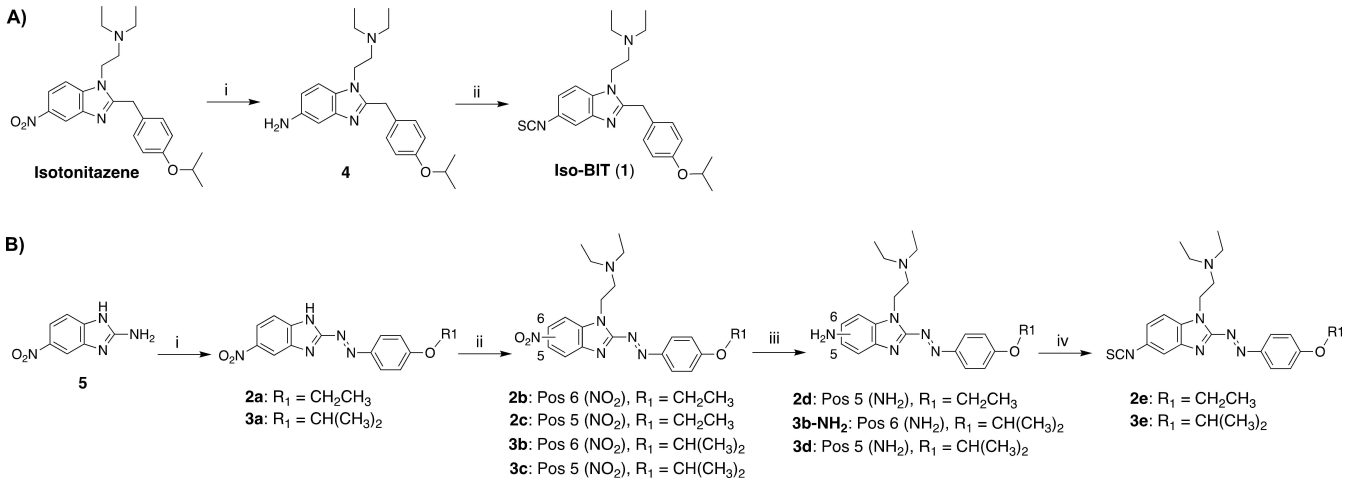

Figure 2. Synthesis of Iso-BIT (**1**) and photochromic nitazenes, with series **2** modeled on etonitazene/BIT and series **3** modeled on isotonitazene/Iso-BIT. A) Synthesis of Iso-BIT (**1**). (i) isotonitazene, H_2, Pd/C, methanol, rt, 3 h, to yield **4**, which was directly used in next step; (ii) CS_2, Et_3N, THF, N_2, 0 °C → rt, 18 h, then TsCl, 0 °C → rt, 1 h, 29% overall yield. B) Synthesis of photochromic nitazene derivatives. (i) 5-nitro-1*H*-benzimidazol-2-ylamine (**5**), 4-ethoxyaniline, DBU, N-chlorosuccinimide, DCM, −78 °C, 0.5 h, 13% (**2a**) or 8% (**3a**); (ii) 2-chloro-*N*,*N*-diethylethylamine hydrochloride, KOH, K_2CO_3, acetone, reflux, 3 h, 22% (**2b**), 16% (**2c**), 26% (**3b**) or 23% (**3c**); (iii) H_2, Pd/C, methanol, rt, 3 h, 52% (**2d**), 8% (**3b-NH$_2$**) or 33% (**3d**); (iv) CS_2, Et_3N, THF, N_2, 0 °C → rt, 18 h, then TsCl, 0 °C → rt, 1 h, 49% (**2e**) or 48% (**3e**).

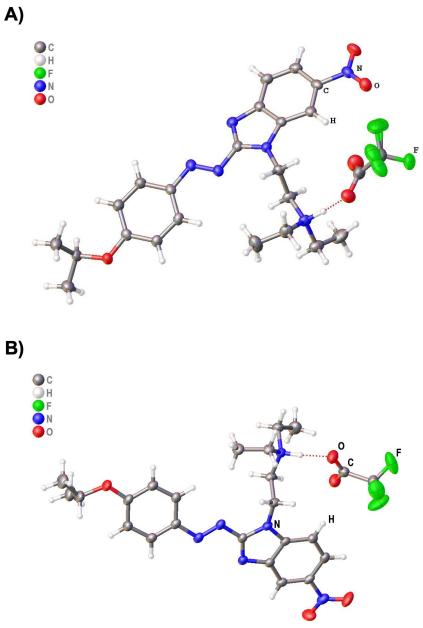

Figure 3. Crystal structure of A) isopropoxy **3b** (CCDC 2236462) and B) Isopropoxy **3c** (CCDC 2236450), both as TFA salts, shown as a 3D ball-and-stick representation.

stabilities of respective *cis*-isomers (Figure 4, Table 1 and Supporting Information). Compounds in both series **2** and **3** were successfully able to reversibly isomerize between *trans*- and *cis*-isomers, except for compounds **2d**, **3d** and **3b-NH$_2$**. The latter derivatives differ from the former in that they contain an amine group at position 5 or 6 of the benzimidazole unit instead of hydrogen, nitro or isothiocyanate groups. In UV/Vis absorption measurements, these amine-containing derivatives each displayed an absorbance band that spanned from approximately 300 to 600 nm in both DMSO and buffer solutions (see Supporting Information). To obtain the respective *cis*-isomers, compounds **2d**, **3d** and **3b-NH$_2$** were separately exposed to light of various wavelengths ranging from 265 to 745 nm and were continuously monitored by online UV/Vis measurements; however, no prominent changes in absorbance were observed compared to their respective thermal equilibrium spectra. These results suggested that the switching properties of the amine-containing derivatives could not be monitored or observably controlled under the described parameters.

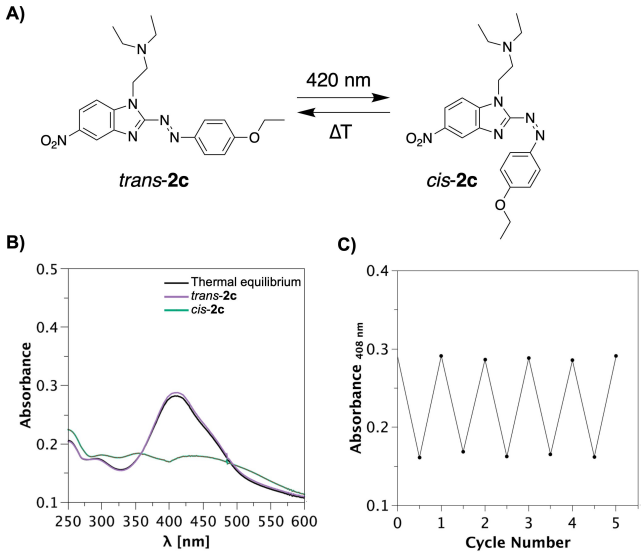

Figure 4. Light-induced isomerization and cycle performance of compound **2c**. This molecule is shown here as a representative, as most compounds in both series **2** and **3** exhibited similar properties (see Supporting Information). A) Depiction of the structural changes that ensue upon photo-induced isomerization of **2c**. B) Online UV/Vis absorption spectra of thermal equilibrium, *trans*-isomer and *cis*-isomer. The *cis*-isomer was accessed via continuous irradiation at 420 nm, while the *trans*-isomer was obtained thermally under dark conditions. C) Cycle performance of **2c** was assessed under alternating conditions of irradiation and darkness. Data points were recorded at the absorbance maximum of the respective *trans*-isomer (408 nm). Results are shown of **2c** (20 μM) in buffer solution (TrisHCl Buffer, pH 7.5) + 0.2 % DMSO at 25 °C.

Despite different substitution patterns, the UV/Vis absorption spectra of the lead photoswitchable derivatives were relatively similar, with a slight bathochromic shift observed for compounds that contained an N-substitution on the benzimidazole core (**2b**, **2c**, **2e**, **3b**, **3c** and **3e**, compared to **2a** and **3a**, see Supporting Information). The similarity observed may be attributed to the strong electron-donating properties of the ethoxy (series **2**) and isopropoxy groups (series **3**) on the benzene unit, potentially outweighing the synthetic variations among compounds, which primarily are only differences in the electron-withdrawing properties of the benzimidazole unit.

The presence of electron-donating and electron-withdrawing groups on opposing sides of the azo unit induces a phenomenon known as the 'push-pull' effect. This effect has been shown to influence *cis*-isomer thermal stabilities, as well as π→π* and/or n→π* transitions.[28] Unlike typical azobenzenes, which require UV or near-UV irradiation to excite their π→π* transitions,[17c,28c] the lead 2-benzimidazole azo-arenes exhibited desirable red-shifted π→π* transitions, as observed in the corresponding UV/Vis absorption spectra. Consequently, visible-light irradiation of 420 nm could be used to excite this transition and obtain the respective *cis*-isomers for all lead compounds, namely **2a**, **2b**, **2c**, **2e**, **3a**, **3b**, **3c** and **3e**. Since UV irradiation can be toxic to most biological material,[17b] the ability to use blue light (420 nm) instead of UV irradiation can be considered less harmful and promising for the use of these molecules as biochemical probes. Since an overlap of the π→π* and n→π* transitions were observed for the 2-benzimidazole azo-arenes described herein, quantitative switching was not obtained (Figure 4 and Table 1). PSS estimations indicated that *cis*-isomeric states constituted 45–80 % *cis*-isomer in buffer solution (Table 1). Despite these findings, previous studies have reported non-quantitative photoswitchable ligands that displayed biological differences between isomers, therefore, the biological activity of these nitazene molecules still remained of interest.[29]

While no clear correlation could be made between the described substitution patterns and corresponding PSS values, thermal stability measurements proved insightful (Table 1 and Supporting Information). Fast thermal relaxations (5–65 sec), from *cis*- to *trans*-isomeric states, were obtained in buffer solution for the tested 2-benzimidazole azo-arenes (Table 1). In these

Table 1. Summary of photophysical properties in buffer solution.[a,b]

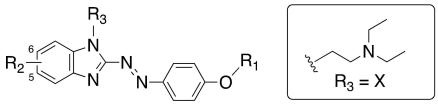

Compound	R_1	R_2	R_3	PSS[c] TE *trans*:*cis*	PSS[c] TE → *cis* *trans*:*cis*	$t_{1/2}$ [s]
2a	CH_2CH_3	NO_2	H	76:24	36:64	46.2
2b	CH_2CH_3	6-NO_2	X	80:20	37:63	6.9
2c	CH_2CH_3	5-NO_2	X	97:3	34:66	10.8
2e	CH_2CH_3	5-NCS	X	83:17	52:48	15.1
3a	$CH(CH_3)_2$	NO_2	H	76:24	55:45	65.4
3b	$CH(CH_3)_2$	6-NO_2	X	72:28	37:63	5.2
3c	$CH(CH_3)_2$	5-NO_2	X	93:7	20:80	15.5
3e	$CH(CH_3)_2$	5-NCS	X	92:8	55:45	15.1

[a] Isomerization was achieved by 5 second irradiation at 420 nm (for *cis*-isomer) or thermally under dark conditions (for *trans*-isomer) at 25 °C. [b] Buffer solution (TrisHCl Buffer, pH 7.5) + 0.2–1 % DMSO. [c] PSS was estimated from UV/Vis absorption spectroscopy data. TE refers to thermal equilibrium.

experiments, differences could be observed between compounds containing an N-diethylaminoethyl unit (**2b**, **2c**, **2e**, **3b**, **3c** and **3e**) and those lacking the N-substituent (**2a** and **3a**). The *cis*-isomers of the latter group displayed thermal half-lives of 46.2 and 65.4 sec, respectively, while that of the remaining compounds ranged from 5.2 to 15.5 sec. The higher thermal stability of *cis*-**2a** and *cis*-**3a** may be attributed to the absence of the N-substituent, revealing a secondary amine on the benzimidazole unit. The secondary amine may reduce electron withdrawing effects, and thus, slightly diminish the push-pull effects responsible for lower thermal stabilities. These results were more pronounced in DMSO studies (SI Table 1). In DMSO studies, the *cis*-isomers of ethoxy **2a** and isopropoxy **3a** exhibited thermal half-lives of 3.2 and 2.1 h, respectively, while the *cis*-isomers of the remaining compounds in series **2** ranged from 0.9 to 1.5 h and that of series **3** ranged from 18.1 to 32.6 min. These results suggested that 2-benzimidazole azo-arenes, like other arylazoheterocycles, may be susceptible to photophysical variations with only slight chemical modifications. The impacts of different solvents, including DMSO and water, on *cis*-isomer thermal stabilities have been previously investigated for phenylazoindole photoswitches.[30] In the context of this work, the photophysical properties in buffer solution were of major interest as these nitazene probes were subjected to cell-based assays to evaluate compound affinity and activity toward the μOR. While fast-relaxing systems may be valuable for a variety of material and biochemical applications,[31] continuous irradiation with blue light was required to evaluate the biochemical properties of these nitazene derivatives. To facilitate this evaluation, a 96-well plate LED device was specifically developed, enabling continuous irradiation of individual wells in cell-based experiments. Due to the fast-switching nature of the *cis*-isomers in buffer solution, the *trans*-isomers of these photoswitchable nitazenes could be obtained thermally. Accordingly, for biochemical investigations, dark conditions were employed to obtain *trans*-enriched isomeric states, while continuous 420 nm irradiation was employed to obtain *cis*-enriched isomeric states.

The lead photoswitchable derivatives **2a**, **2b**, **2c**, **2e**, **3a**, **3b**, **3c** and **3e** were subjected to radioligand binding studies to assess their affinity for the μOR (Table 2). These ligands were evaluated in their inherent thermal equilibrium state, predominantly comprising the *trans*-isomer, to screen for biochemically-relevant compounds. Reference compounds in these investigations included fentanyl, isotonitazene, BIT and the newly synthesized Iso-BIT. In this system, isotonitazene (K_i = 0.95 nM) displayed a binding affinity that was 9-fold greater than fentanyl (K_i = 8.3 nM). These results were consistent to previously reported functional studies that describe a 9-fold greater potency for isotonitazene than fentanyl.[4,8e] While BIT (K_i = 40 nM) and Iso-BIT (K_i = 27 nM) displayed attenuated binding affinities compared to isotonitazene, the replacement of nitro by isothiocyanate still yielded affinity in the nM range, remaining within an ideal affinity range.

For the nitro-containing photoswitchable ligands (**2a**–**c** and **3a**–**c**), the methylene group characteristic for etonitazene and isotonitazene was substituted with an azo group. This exchange did not yield strong affinities toward the μOR for compounds **2a**–**c** and **3a**–**c**, with K_i values ranging from 720 to 10000 nM. Furthermore, no specific trend could be discerned between these nitro-containing derivatives. Interestingly, the isothiocyanate-containing derivatives exhibited slightly superior binding properties, with *trans*-**2e** (K_i = 580 nM) and *trans*-**3e** (K_i = 620 nM) displaying the highest affinities among all photochromic nitazenes, in the submicromolar range. Despite predominantly suboptimal initial results, we pursued functional assays to explore the structure-activity relationship between these nitazenes and the μOR, which proved insightful.

Table 2. Binding affinities of *trans*-enriched photoswitchable ligands and reference compounds to the human μOR, derived from radioligand binding studies.[a]

Photoswitchable Compounds:

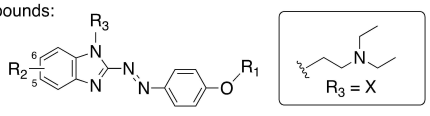

Compound				μOR_{wt}	
				K_i [nM ± S.E.M.][b]	(n)[c]
Non-Photoswitchable Compounds					
Fentanyl				8.3 ± 1.5	11
Isotonitazene				0.95 ± 0.31	6
BIT				40 ± 6.6	5
Iso-BIT				27 ± 8.7	4
Photoswitchable Compounds					
	R_1	R_2	R_3		
trans-**2a**	CH_2CH_3	NO_2	H	10000 ± 4200[d]	2
trans-**2b**	CH_2CH_3	6-NO_2	X	1700 ± 220	4
trans-**2c**	CH_2CH_3	5-NO_2	X	1100 ± 220	5
trans-**3a**	$CH(CH_3)_2$	NO_2	H	720 ± 130[d]	2
trans-**3b**	$CH(CH_3)_2$	6-NO_2	X	970 ± 190[d]	2
trans-**3c**	$CH(CH_3)_2$	5-NO_2	X	800 ± 420 [d]	2
Covalent Photoswitchable Compounds					
trans-**2e**	CH_2CH_3	5-NCS	X	580 ± 130	4
trans-**3e**	$CH(CH_3)_2$	5-NCS	X	620 ± 28[d]	2

[a] Binding to the μOR was determined using membrane preparations from HEK293T cells transiently transfected with μOR and the radioligand [^{3}H]diprenorphine. In the case of irreversible interactions, K_i refers to pseudo-K_i. [b] Mean K_i values in [nM ± S.E.M.] were derived from 3–11 individual experiments, each performed in triplicate. [c] Number of individual experiments. [d] Mean K_i ± SD from two individual experiments.

Ligand-mediated receptor activation was assessed via a biosensor-based BRET assay in HEK293T cells that were transiently transfected with human μOR.[32] Each photoswitchable ligand was irradiated at 420 nm for the full duration of incubation or was subjected to dark conditions to obtain either the respective *cis*- or *trans*-enriched isomeric state (Figure 5 and Table 3). The agonist fentanyl and the nitazenes isotonitazene, BIT and Iso-BIT were evaluated for comparison. To examine whether continuous irradiation would interfere with the cellular assay, fentanyl and isotonitazene were additionally subjected to 420 nm irradiation. In this activation assay, isotonitazene behaved as a full agonist (E_{max} = 105 %) with an EC_{50} value of 11 nM, which was comparable to that of fentanyl (EC_{50} = 6.0 nM). This finding contrasts with the obtained K_i values that indicate a 9-fold higher binding affinity for isotonitazene than fentanyl and differs from previously reported functional studies, which indicate that the potency of isotonitazene is 9-fold higher in both β-arrestin 2 (EC_{50} = 1.6 nM) and mini-G_i recruitment assays (EC_{50} = 3.7 nM) than that of fentanyl (EC_{50} = 14 and 35 nM, respectively).[4] Nevertheless, results from the biosensor-based BRET assay validate that isotonitazene exhibits powerful potency in the nM range.

Replacing the 5-NO_2 group in isotonitazene with 5-NCS caused a 16-fold reduction in potency for Iso-BIT, resulting in an EC_{50} value of 180 nM. This finding is consistent with literature that describes a poorer potency for BIT (5-NCS) than etonitazene (5-NO_2).[4,11a] In comparison to Iso-BIT, the ethoxy-containing BIT exhibited a higher potency of 63 nM. When interpreting these findings, it is important to note that the isothiocyanates were specifically designed to form stable and non-easily displaceable covalent bonds with the target receptor, in contrast to the freely-diffusible etonitazene and isotonitazene. As a result, achieving potencies in the nM range can be deemed noteworthy, particularly when considering their capability to function as full efficacy agonists (E_{max} = 98 % for Iso-BIT and 93 % for BIT).

For biochemical evaluations of the photoswitchable nitazene derivatives, continuous irradiation throughout the assay was required to maintain the respective *cis*-isomers. As displayed in Figure 5 and Table 3, fentanyl and isotonitazene exhibited similar functional behavior when exposed to 420 nm irradiation and when kept in the dark (fentanyl: EC_{50} = 6.0 nM vs fentanyl [420 nm]: EC_{50} = 6.3 nM; isotonitazene: EC_{50} = 11 nM vs isotonitazene [420 nm]: EC_{50} = 15 nM). This finding indicates that the employed irradiation conditions were compatible with the biosensor-based BRET assay. When evaluating the photoswitchable ligands **2a**–**c** and **3a**–**c**, a strong structure-dependent activation profile could be discerned (Figure 5 and Table 3). For *trans*-**2a** and *trans*-**3a**, which lack the N-diethylaminoethyl group, no explicit stimulation of the receptor could be measured up to a concentration of 10 μM. This result is in good agreement with literature that suggests the N-diethylaminoethyl substituent on the benzimidazole core to be important for μOR-nitazene interactions.[8c] Moreover, receptor activation substantially increased for compounds that contain this N-substituent, with the best activation profiles observed for *trans*-**2c** (EC_{50} = 280 nM and E_{max} = 62 %) and *trans*-**3b** (EC_{50} = 250 nM and E_{max} = 60 %). Regarding the positioning of the nitro group, previous reports have indicated that the nitro group at position 5 in etonitazene offers improved μOR-mediated analgesic effects compared to when it is placed at position 6.[3,8b,c] While this trend could be observed for the ethoxy series, the isopropoxy derivative *trans*-**3b** (6-NO_2) emerged as the superior isopropoxy analogue. Discrepancies may be attributed to differences in potency between the photochromic nitazenes and previously reported nitazenes. Comparing the activation data of the respective *trans*- and *cis*-isomers of the photoswitchable ligands revealed that both isomer-enriched states behaved similarly in activating the μOR (Figure 5; light blue and dark blue curves, respectively). The most pronounced difference between both isomers could be observed for **2b**. While *cis*-**2b** displayed weak efficacy (E_{max} = 12 %) and poor potency (EC_{50} = 1400 nM), partial agonist activity and a 2-fold higher potency could be observed for *trans*-**2b** as exhibited by an E_{max} value of 39 % and an EC_{50} value of 630 nM.

The isothiocyanates **2e** and **3e** could not be measured in this assay as the detection signal was substantially diminished to more than 100 % below basal activity at concentrations greater than 3 μM. This observation may be explained by an interference

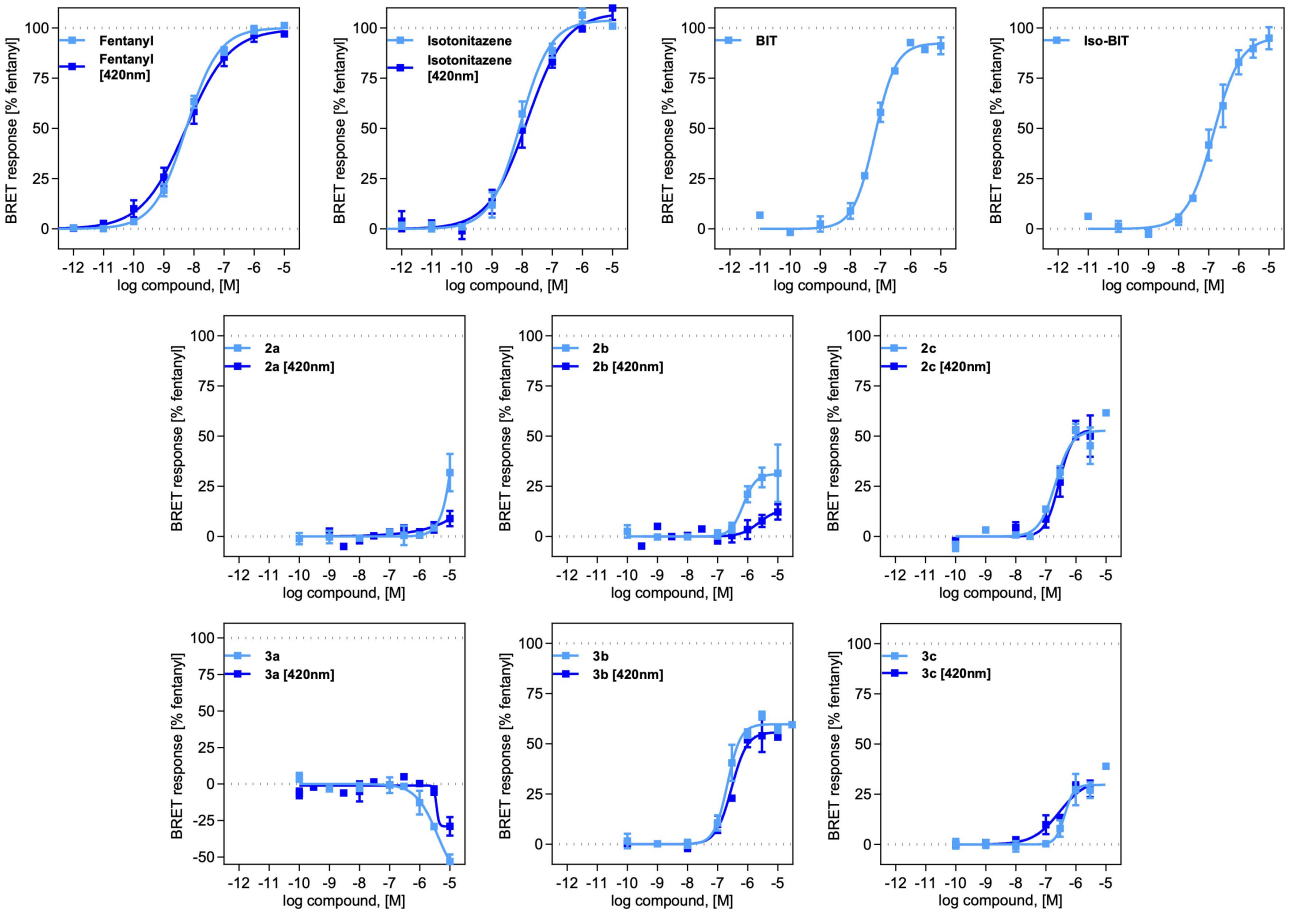

Figure 5. Activation of the μOR by synthetic opioids measured via a biosensor-based BRET assay. Receptor activation was evaluated for isotonitazene, BIT and Iso-BIT, as well as for the non-covalent (**2a–c** and **3a–c**) and covalent (**2e** and **3e**) photoswitchable compounds, in HEK293T cells transiently co-transfected with μOR and the hybrid G-protein $G\alpha_{qi5HA}$ (light blue curves). To measure the activating effect of the *cis*-isomers, cells were continuously irradiated at 420 nm for the full duration of the experiment (dark blue curves). As a control to evaluate any influence of irradiation on signaling outputs, fentanyl and isotonitazene were subjected to the same irradiation conditions as that to obtain the respective *cis*-isomers (fentanyl [420 nm], isotonitazene [420 nm]; dark blue curves). Graphs show mean curves (± S.E.M.) of 3–7 individual experiments, each performed in duplicate.

of these isothiocyanate derivatives with the BRET detection system. While the BRET system measures receptor activation at equilibrium by monitoring G-protein dissociation, a FRET-based second messenger accumulation assay (IP-One® assay) was employed as an alternative test system to evaluate nitazenes **2e** and **3e**. Furthermore, it was of interest to corroborate the obtained receptor activation data for the other nitazenes under alternative experimental conditions. The IP accumulation assay was performed with HEK293T cells that were transiently co-transfected with human μOR and the hybrid G-protein $G\alpha_{qi5HA}$ (Figure 6 and Table 3).[33] The *trans*-isomers of **2a–c**, **2e**, **3a–c** and **3e** were evaluated in the dark, while their respective *cis*-isomers were evaluated under continuous irradiation at 420 nm. For comparison, receptor activation of fentanyl and isotonitazene (both in the dark and at 420 nm), as well as BIT and Iso-BIT, was determined. Apart from isotonitazene, these compounds exhibited comparable potencies, falling within a 2-fold range, to that obtained in the BRET system. Isotonitazene, on the other hand, showed a 4-fold higher potency in the IP accumulation system as indicated by an EC_{50} value of 2.8 nM.

Overall, the photoswitchable nitazenes exhibited similar structure-dependent activation trends to those discerned in the BRET system, however, with a 3- to 11-fold reduction in potency. The 5-nitro derivative *trans*-**2c** exhibited the best activation profile in the ethoxy series with an EC_{50} value of 2000 nM. In the isopropoxy series, however, both *trans*-**3b** (6-nitro) and *trans*-**3c** (5-nitro) displayed the highest potencies with EC_{50} values of 2300 nM and 2100 nM, respectively. Regarding μOR efficacy, the *trans*-enriched states of **2c**, **3b** and **3c** each behaved as full agonists with E_{max} values of 99%, 105% and 103%, respectively. In contrast, the isothiocyanates **2e** and **3e** exhibited only partial agonist activity with E_{max} values of 32% for *cis*-**2e** (EC_{50} = 3800 nM) and 60% for *cis*-**3e** (EC_{50} = 10000 nM). Interestingly, activity differences between the respective *cis*- and *trans*-isomers of **2e** and **3e** could be observed (Figure 6 and Table 3), whereby the *cis*-isomers exhibited slightly superior activation profiles.

In addition to assessing the functional properties of these NCS-containing ligands, it was of major interest to evaluate their ability to covalently interact with the μOR. To determine this, a radioligand depletion assay was employed,[34] using membranes of HEK293T cells that transiently express μOR. Covalent inter-

Table 3. Activation of the μ-opioid receptor (μOR) by synthetic opioids.[a]

Photoswitchable Compounds:

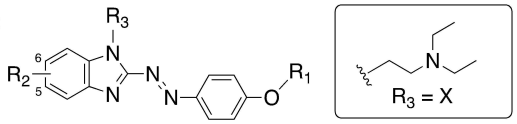

Compound				Biosensor-based BRET assay (μOR_{wt})			IP-One assay (μOR_{wt})		
				EC_{50} [nM ± S.E.M.][b]	E_{max} [% ± S.E.M.][c]	(n)[d]	EC_{50} [nM ± S.E.M.][b]	E_{max} [% ± S.E.M.][c]	(n)[e]
Non-Photoswitchable Compounds									
Fentanyl				6.0 ± 1.0	100	7	3.7 ± 1.2	100	4
Fentanyl [420 nm]				6.3 ± 1.9	100 ± 2	3	6.8 ± 2.1	101 ± 2	7
Isotonitazene						11 ± 4.1	105 ± 3	5	4
Isotonitazene [420 nm]				15 ± 5.5	104 ± 2	3	3.7 ± 0.66	97 ± 4	4
BIT				63 ± 13	93 ± 2	3	64 ± 19	95 ± 2	4
Iso-BIT				180 ± 75	98 ± 6	3	190 ± 48	93 ± 1	3
Photoswitchable Compounds									
	R_1	R_2	R_3						
trans-**2a**	CH_2CH_3	NO_2	H	n/q	32 ± 9[f]	3	n/q	10 ± 5[f]	3
cis-**2a**	CH_2CH_3	NO_2	H	n/q	9 ± 4[f]	3	n/q	11 ± 3[f]	3
trans-**2b**	CH_2CH_3	6-NO_2	X	630 ± 150	39 ± 9	4	7100 ± 2200	68 ± 7	3
cis-**2b**	CH_2CH_3	6-NO_2	X	1400 ± 830	12 ± 4	4	8300 ± 1400	52 ± 9	3
trans-**2c**	CH_2CH_3	5-NO_2	X	280 ± 31	62 ± 5	4	2000 ± 430	99 ± 1	4
cis-**2c**	CH_2CH_3	5-NO_2	X	410 ± 64	67 ± 4	3	2700 ± 630	96 ± 3	7
trans-**3a**	$CH(CH_3)_2$	NO_2	H	n/q	< 0	3	n/q	−12 ± 6[f]	3
cis-**3a**	$CH(CH_3)_2$	NO_2	H	n/q	< 0	3	n/q	−18 ± 3[f]	3
trans-**3b**	$CH(CH_3)_2$	6-NO_2	X	250 ± 46	60 ± 1	4	2300 ± 790	105 ± 4	5
cis-**3b**	$CH(CH_3)_2$	6-NO_2	X	340 ± 130	57 ± 5	3	3600 ± 1200	100 ± 3	5
trans-**3c**	$CH(CH_3)_2$	5-NO_2	X	540 ± 140	40 ± 4	4	2100 ± 1700	103 ± 7	3
cis-**3c**	$CH(CH_3)_2$	5-NO_2	X	470 ± 280	35 ± 5	4	1500 ± 260	83 ± 6	8
Covalent Photoswitchable Compounds									
trans-**2e**	CH_2CH_3	5-NCS	X	n/a	n/a	3	n/q	13 ± 5[f]	3
cis-**2e**	CH_2CH_3	5-NCS	X	n/a	n/a	2	3800 ± 1400	32 ± 2	4
trans-**3e**	$CH(CH_3)_2$	5-NCS	X	n/a	n/a	3	n/q	18 ± 4[f]	3
cis-**3e**	$CH(CH_3)_2$	5-NCS	X	n/a	n/a	2	10000 ± 3800	60 ± 6	4

[a] μOR activation was determined via either a biosensor-based BRET assay or the IP-One accumulation assay (Cisbio). [b] Potency for μOR activation is shown as mean EC_{50} in [nM ± S.E.M.]. [c] Mean value for maximum efficacy is reported as E_{max} in [% ± S.E.M.] relative to the full effect of fentanyl. [d] Number of individual experiments conducted in duplicate. [e] Number of individual experiments conducted in triplicate. [f] Efficacy at 10 μM. The abbreviation n/q refers to 'not quantifiable', while n/a refers to 'not applicable'.

action at the μOR orthosteric binding site was evaluated time-dependently by incubating the receptor with either isothiocyanate **2e** or **3e** in their thermal equilibrium state, or with the negative control isotonitazene, for durations of 5, 15, 30 or 60 min (Figure 7 and SI Table 2). At the end of the treatment, reversibly-bound ligands were carefully washed from the receptor and membranes were incubated with the radioligand [^{3}H]diprenorphine. The amount of specific binding of radioligand indicated the number of accessible binding sites, and consequently, the extent of covalent binding. Remarkably, both azo-containing isothiocyanates **2e** and **3e** displayed a strong and fast covalent interaction with the μOR, exhibiting a covalent binding maximum of 96% and 94%, respectively.

In a comparative study, the methylene-bearing nitazene BIT and its analogue Iso-BIT were tested under the same conditions (Figure 7 and SI Table 2). Interestingly, both BIT and Iso-BIT were only able to partially block the μOR, exhibiting a covalent binding maximum of 53% (BIT) and 58% (Iso-BIT) after 60 min. These results are somewhat comparable to studies that were performed in 1983 with rat brain membranes, which suggested BIT to covalently bind to 45% of μOR after a 30-min incubation period.[9]

Overall, these findings indicate that BIT and iso-BIT exhibit substantially poorer covalent binding properties than the azo-containing derivatives **2e** and **3e**. The superior properties of these latter compounds become more pronounced when

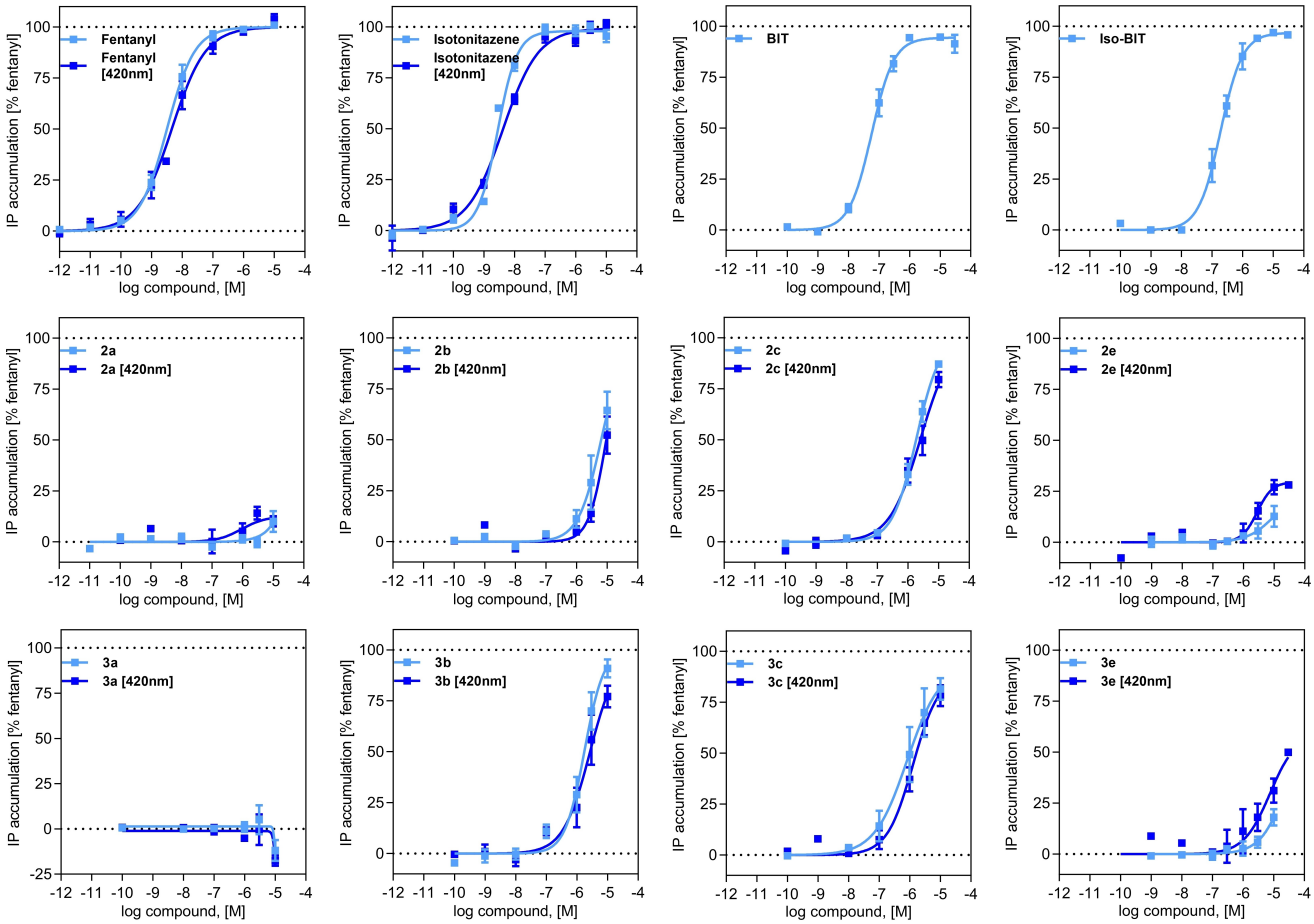

Figure 6. Activation of the μOR by synthetic opioids measured via the IP-One® accumulation assay. G-protein-mediated μOR activation was investigated for isotonitazene, BIT and Iso-BIT, as well as for the non-covalent (**2a–c** and **3a–c**) and covalent (**2e** and **3e**) photoswitchable compounds, in HEK293T cells transiently co-transfected with μOR and the hybrid G-protein $G\alpha_{qi5HA}$ (light blue curves). The activating effect of the *cis*-isomers was determined under continuous irradiation at 420 nm (dark blue curves). As a control, fentanyl and isotonitazene were similarly subjected to continuous irradiation at 420 nm (fentanyl [420 nm], isotonitazene [420 nm]; dark blue curves). Graphs show mean curves (± S.E.M.) of 3–8 individual experiments, each performed in triplicate.

evaluating the kinetics of this reaction (SI Table 2). For **2e** and **3e**, the covalent binding half-life ($t_{1/2}$) was determined to be 3 min and 4 min, respectively, resulting in 96% (**2e**) and 94% (**3e**) of receptors being blocked after only a 5-min incubation period. In contrast, BIT and Iso-BIT both displayed a $t_{1/2}$ of 17 min. These findings establish **2e** and **3e** as attractive μOR ligands that can effectively localize and covalently bind to the orthosteric binding site of the μOR at physiological pH.

Conclusions

Nitazenes represent an underexplored class of potent μOR ligands that are receiving increased attention. To advance nitazene-based probes for future investigations of the μOR and to explore new active ligands targeting this receptor, photoswitchable derivatives were developed. The successful synthesis of these molecules allowed for photophysical evaluations of 2-benzimidazole azo-arenes, revealing a novel photoswitchable scaffold that isomerizes when exposed to visible light in both DMSO and buffer solutions.

Substituting the methylene group present in etonitazene and isotonitazene with a photoswitchable azo group maintained agonist properties but reduced the potency for **2a–c** and **3a–c** toward the μOR in two different G-protein signaling assays. Furthermore, no profound functional differences between the respective *trans*- and *cis*-isomers could be discerned in these assays. The biochemical results became particularly noteworthy when assessing ligands that contain an isothiocyanate functionality designed for covalent interaction with the μOR. The investigated ligands included the previously documented nitazene BIT and the newly synthesized iso-BIT, as well as the azo-containing derivatives **2e** and **3e**. The former isothiocyanates behaved as full efficacy agonists with nM potencies, while the latter derivatives exhibited partial agonism at higher concentrations. Remarkably, both **2e** and **3e** were able to form an exceptionally high fraction (>90%) of covalent ligand-receptor complexes with wild-type μOR after only a 5-min incubation period. This finding was particularly impressive compared to the results of BIT and iso-BIT, which showed covalent binding maxima of 53% and 58%, respectively. Even though further investigations must be conducted to ascertain the exact μOR

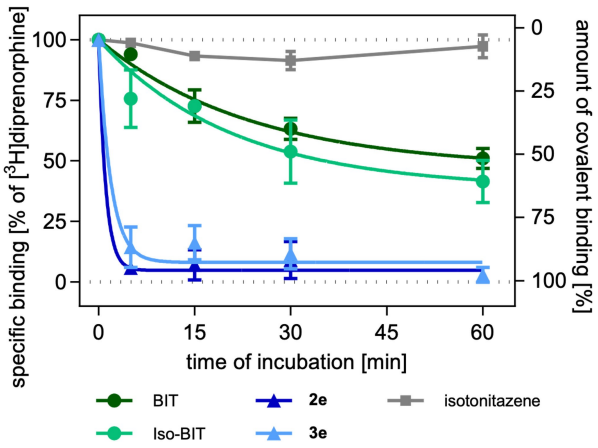

Figure 7. Covalent binding of NCS-containing nitazene compounds to wild-type μOR. Covalent binding of full efficacy agonists BIT and Iso-BIT, as well as azo-containing ligands **2e** and **3e** in their thermal equilibrium state, was determined in a [^{3}H]diprenorphine radioligand depletion assay with homogenates from HEK293T cells expressing the human μOR. Results were compared to those obtained using the reversible ligand isotonitazene. BIT and Iso-BIT displayed covalent binding of 53% and 58%, respectively, while near-complete blocking (greater than 90%) was obtained for **2e** and **3e** after only a 5-min incubation period. All test compounds were evaluated at a concentration 30- to 50-fold higher than their respective K_i values (BIT (2 μM), Iso-BIT (1 μM), **2e** (20 μM), **3e** (20 μM) and isotonitazene (50 nM)). Graphs show mean curves (± S.E.M.) of 3 individual experiments, each performed in quadruplicate.

residues involved in this interaction, **2e** and **3e** could effectively localize and covalently bind to the orthosteric binding site of μOR at physiological pH.

Overall, these findings exhibit the versatile nature of nitazenes, demonstrating their ability to function as partial or full efficacy agonists and behave as either freely-diffusible or covalent ligands with only minor chemical modifications. Further exploration of nitazenes, both chemically and biologically, may not only grant access to a diverse range of μOR-targeting ligands but also be essential in understanding their impressive interactions with the μOR, ultimately advancing our understanding of this medically-relevant receptor.

Supporting Information

The authors have cited additional references within the Supporting Information.[35]

Acknowledgements

This work was supported by the Deutsche Forschungsgemeinschaft, RTG 1910 and a Minerva PhD Fellowship to RL. We thank Julia Zach for assistance in developing the 96-well plate LED device. Open Access funding enabled and organized by Projekt DEAL.

Conflict of Interests

The authors declare no conflict of interest.

Data Availability Statement

The data that support the findings of this study are available from the corresponding author upon reasonable request.

Keywords: covalent · isotonitazene · μ-opioid receptor · G-protein-coupled receptor · photopharmacology

[1] a) EMCDDA, Report on the risk assessment of N,N-diethyl-2- [[4-(1-methylethoxy)phenyl]methyl]-5-nitro-1H- benzimidazole-1-ethanamine (isotonitazene) in accordance with Article 5c of Regulation (EC) No 1920/2006 (as amended), https://www.emcdda.europa.eu/publications/risk-assessments/isotonitazene_en, 2020. Accessed 01 Feb 2023; b) European Commission, Commission Delegated Directive (EU) 2020/1687 of 2 September 2020 amending the Annex to Council Framework Decision 2004/757/JHA as regards the inclusion of the new psychoactive substance N,N-diethyl-2-[[4-(1-methylethoxy)phenyl]methyl]-5-nitro-1H-benzimidazole-1-ethanamine (isotonitazene) in the definition of 'drug', http://data.europa.eu/eli/dir_del/2020/1687/oj, 2020. Accessed 01 Feb 2023.
[2] a) A. J. Krotulski, D. M. Papsun, S. L. Kacinko, B. K. Logan, *J. Anal. Toxicol.* **2020**, *44*, 521–530; b) WHO, Critical Review Report: ISOTONITAZENE, https://www.who.int/docs/default-source/controlled-substances/43rd-ecdd/isonitazene-43rd-final-complete-a.pdf, 2020. Accessed 01 Feb 2023.
[3] A. Hunger, J. Kebrle, A. Rossi, K. Hoffmann, *Helv. Chim. Acta* **1960**, *43*, 1032–1046.
[4] M. M. Vandeputte, K. Van Uytfanghe, N. K. Layle, D. M. St Germaine, D. M. Iula, C. P. Stove, *ACS Chem. Neurosci.* **2021**, *12*, 1241–1251.
[5] A. Hunger, J. Kebrle, A. Rossi, K. Hoffmann, *Experientia* **1957**, *13*, 400–401.
[6] United Nations, 17. Protocol amending the Single Convention on Narcotic Drugs, 1961. Geneva, 25 March 1972, https://treaties.un.org/Pages/ViewDetails.aspx?src=IND&mtdsg_no=VI-17&chapter=6&clang=_en, 1975. Accessed 01 Feb 2023.
[7] a) F. Mueller, C. Bogdal, B. Pfeiffer, L. Andrello, A. Ceschi, A. Thomas, E. Grata, *Forensic Sci. Int.* **2021**, *320*, 110686; b) M. M. Vandeputte, M. M. Tsai, L. Chen, G. C. Glatfelter, D. Walther, C. P. Stove, L. Shi, M. H. Baumann, *Drug Alcohol Depend.* **2023**, *249*, 109939.
[8] a) M. M. Vandeputte, A. Cannaert, C. P. Stove, *Arch. Toxicol.* **2020**, *94*, 3819–3830; b) P. Blanckaert, A. Cannaert, K. Van Uytfanghe, F. Hulpia, E. Deconinck, S. Van Calenbergh, C. Stove, *Drug Test. Anal.* **2020**, *12*, 422–430; c) I. Ujváry, R. Christie, M. Evans-Brown, A. Gallegos, R. Jorge, J. de Morais, R. Sedefov, *ACS Chem. Neurosci.* **2021**, *12*, 1072–1092; d) M. M. Vandeputte, A. J. Krotulski, D. M. Papsun, B. K. Logan, C. P. Stove, *J. Anal. Toxicol.* **2021**, *46*, 115–121; e) M. A. De Luca, G. Tocco, R. Mostallino, A. Laus, F. Caria, A. Musa, N. Pintori, M. Ucha, C. Poza, E. Ambrosio, G. Di Chiara, M. P. Castelli, *Neuropharmacology* **2022**, *221*, 109263; f) P. Skolnick, *Pharmacol. Ther.* **2022**, *233*, 108019; g) K. Hasegawa, K. Minakata, M. Suzuki, O. Suzuki, *Forensic Toxicol.* **2022**, *40*, 234–243; h) A. L. A. Mohr, B. K. Logan, M. F. Fogarty, A. J. Krotulski, D. M. Papsun, S. L. Kacinko, M. A. Huestis, J. D. Ropero-Miller, *J. Anal. Toxicol.* **2022**, *46*, e116–e185; i) T. Kanamori, Y. Okada, H. Segawa, T. Yamamuro, K. Kuwayama, K. Tsujikawa, Y. T. Iwata, *Drug Test Anal.* **2023**, *15*, 449–457.
[9] K. C. Rice, A. E. Jacobson, T. R. Burke Jr., B. S. Bajwa, R. A. Streaty, W. A. Klee, *Science* **1983**, *220*, 314–316.
[10] D. Weichert, P. Gmeiner, *ACS Chem. Biol.* **2015**, *10*, 1376–1386.
[11] a) T. R. Burke Jr., B. S. Bajwa, A. E. Jacobson, K. C. Rice, R. A. Streaty, W. A. Klee, *J. Med. Chem.* **1984**, *27*, 1570–1574; b) T. R. Burke Jr, K. C. Rice, A. E. Jacobson, W. F. Simonds, W. A. Klee, *J. Labelled Compd. Radiopharm.* **1984**, *21*, 693–702; c) S. McLean, R. B. Rothman, A. E. Jacobson, K. C. Rice, M. Herkenham, *J. Comp. Neurol.* **1987**, *255*, 497–510; d) R. B. Rothman, V. Bykov, B. R. de Costa, A. E. Jacobson, K. C. Rice, L. S. Brady, *Peptides* **1990**, *11*, 311–331; e) B. Tocque, A. E. Jacobson, K. C. Rice, E. A.

Frey, *Eur. J. Pharmacol.* **1987**, *143*, 127–130; f) J. A. Danks, F. C. Tortella, J. B. Long, V. Bykov, A. E. Jacobson, K. C. Rice, J. W. Holaday, R. B. Rothman, *Neuropharmacology* **1988**, *27*, 965–974; g) Q. Ni, H. Xu, J. S. Partilla, K. C. Rice, D. Matecka, S. N. Calderon, F. Porreca, J. Lai, H. Schmidhammer, R. Krassnig, R. B. Rothman, *Peptides* **1998**, *19*, 1079–1090; h) G. R. Rios, T. R. Tephly, *Drug Metab. Dispos.* **2002**, *30*, 1364–1367; i) R. B. Rothman, V. Bykov, J. A. Danks, A. E. Jacobson, T. R. Burke, K. C. Rice, M. Herkenham, *Neuropeptides* **1985**, *6*, 503–516; j) R. B. Rothman, W. D. Bowen, V. Bykov, U. K. Schumacher, C. B. Pert, A. E. Jacobson, T. R. Burke, K. C. Rice, *Neuropeptides* **1984**, *4*, 201–215; k) R. B. Rothman, J. B. Long, V. Bykov, A. E. Jacobson, K. C. Rice, J. W. Holaday, *Neuropharmacology* **1990**, *29*, 805–810; l) D. J. J. Carr, B. R. DeCosta, C.-H. Kim, A. E. Jacobson, K. L. Bost, K. C. Rice, E. Blalock, *Neuroendocrinology* **2008**, *51*, 552–560; m) J. K. Staley, R. B. Rothman, K. C. Rice, J. Partilla, D. C. Mash, *J. Neurosci.* **1997**, *17*, 8225–8233; n) R. B. Rothman, J. A. Danks, A. E. Jacobson, T. R. Burke, K. C. Rice, C. B. Pert, *Neuropeptides* **1984**, *4*, 311–317; o) H. Xu, J. S. Partilla, B. R. de Costa, K. C. Rice, R. B. Rothman, *Peptides* **1993**, *14*, 893–907; p) R. A. Lessor, B. S. Bajwa, K. C. Rice, A. E. Jacobson, R. A. Streaty, W. A. Klee, C. B. Smith, M. D. Aceto, E. L. May, L. S. Harris, *J. Med. Chem.* **1986**, *29*, 2136–2141; q) S. McLean, R. B. Rothman, D. M. Chuang, K. C. Rice, J. W. Spain, C. J. Coscia, B. L. Roth, *Brain Res. Dev. Brain Res.* **1989**, *45*, 283–289.

[12] J. L. Galzi, A. Mejean, B. Ilien, C. Mollereau, J. C. Meunier, M. Goeldner, C. Hirth, *J. Med. Chem.* **1990**, *33*, 2456–2464.

[13] A. E. Conibear, E. Kelly, *Mol. Pharmacol.* **2019**, *96*, 542–549.

[14] a) J. Shim, A. Coop, A. D. MacKerell Jr., *J. Phys. Chem. B* **2011**, *115*, 7487–7496; b) A. P. Feinberg, I. Creese, S. H. Snyder, *Proc. Natl. Acad. Sci. USA* **1976**, *73*, 4215–4219.

[15] a) Y. Wang, Y. Zhuang, J. F. DiBerto, X. E. Zhou, G. P. Schmitz, Q. Yuan, M. K. Jain, W. Liu, K. Melcher, Y. Jiang, B. L. Roth, H. E. Xu, *Cell* **2023**, *186*, 413–427.e417; b) Q. N. Vo, P. Mahinthichaichan, J. Shen, C. R. Ellis, *Nat. Commun.* **2021**, *12*, 984.

[16] a) E. Bartels, N. H. Wassermann, B. F. Erlanger, *Proc. Nat. Acad. Sci.* **1971**, *68*, 1820–1823; b) M. Izquierdo-Serra, A. Bautista-Barrufet, A. Trapero, A. Garrido-Charles, A. Díaz-Tahoces, N. Camarero, S. Pittolo, S. Valbuena, A. Pérez-Jiménez, M. Gay, A. García-Moll, C. Rodríguez-Escrich, J. Lerma, P. de la Villa, E. Fernández, M. Pericàs, A. Llebaria, P. Gorostiza, *Nat. Commun.* **2016**, *7*, 12221; c) A. Garrido-Charles, A. Huet, C. Matera, A. Thirumalai, J. Hernando, A. Llebaria, T. Moser, P. Gorostiza, *J. Am. Chem. Soc.* **2022**, *144*, 9229–9239; d) R. Lahmy, H. Hübner, D. Lachmann, P. Gmeiner, B. König, *ChemMedChem* **2023**, *18*, e202300228.

[17] a) W. Szymański, J. M. Beierle, H. A. Kistemaker, W. A. Velema, B. L. Feringa, *Chem. Rev.* **2013**, *113*, 6114–6178; b) W. A. Velema, W. Szymanski, B. L. Feringa, *J. Am. Chem. Soc.* **2014**, *136*, 2178–2191; c) M. M. Lerch, M. J. Hansen, G. M. van Dam, W. Szymanski, B. L. Feringa, *Angew. Chem. Int. Ed. Engl.* **2016**, *55*, 10978–10999.

[18] a) L. Welsch, E. Colantonio, M. Frison, D. A. Johnson, S. P. McClain, V. Mathis, M. R. Banghart, S. Ben Hamida, E. Darcq, B. L. Kieffer, *Biol. Psychiatry* **2023**, *94*, 842–851; b) X. Ma, D. A. Johnson, X. J. He, A. E. Layden, S. P. McClain, J. C. Yung, A. Rizzo, J. Bonaventura, M. R. Banghart, *Nat. Methods* **2023**, *20*, 682–685; c) S. P. McClain, X. Ma, D. A. Johnson, C. A. Johnson, A. E. Layden, J. C. Yung, S. T. Lubejko, G. Livrizzi, X. J. He, J. Zhou, J. Chang-Weinberg, E. Ventriglia, A. Rizzo, M. Levinstein, J. L. Gomez, J. Bonaventura, M. Michaelides, M. R. Banghart, *Neuron* **2023**, *111*, 3926–3940; d) M. Schönberger, D. Trauner, *Angew. Chem. Int. Ed. Engl.* **2014**, *53*, 3264–3267; e) R. Lahmy, H. Hübner, M. F. Schmidt, D. Lachmann, P. Gmeiner, B. König, *Chem. Eur. J.* **2022**, *28*, e202201515.

[19] M. J. Fuchter, *J. Med. Chem.* **2020**, *63*, 11436–11447.

[20] a) P. Donthamsetti, N. Winter, A. Hoagland, C. Stanley, M. Visel, S. Lammel, D. Trauner, E. Isacoff, *Nat. Commun.* **2021**, *12*, 4775; b) X. Rovira, A. Trapero, S. Pittolo, C. Zussy, A. Faucherre, C. Jopling, J. Giraldo, J. P. Pin, P. Gorostiza, C. Goudet, A. Llebaria, *Cell Chem. Biol.* **2016**, *23*, 929–934; c) D. Prischich, A. M. J. Gomila, S. Milla-Navarro, G. Sangüesa, R. Diez-Alarcia, B. Preda, C. Matera, M. Batlle, L. Ramírez, E. Giralt, J. Hernando, E. Guasch, J. J. Meana, P. de la Villa, P. Gorostiza, *Angew. Chem. Int. Ed. Engl.* **2021**, *60*, 3625–3631; d) D. Lachmann, R. Lahmy, B. König, *Eur. J. Org. Chem.* **2019**, *2019*, 5018–5024; e) J. Morstein, G. Romano, B. E. Hetzler, A. Plante, C. Haake, J. Levitz, D. Trauner, *Angew. Chem. Int. Ed.* **2022**, *61*, e202117094.

[21] a) J. Calbo, C. E. Weston, A. J. P. White, H. S. Rzepa, J. Contreras-García, M. J. Fuchter, *J. Am. Chem. Soc.* **2017**, *139*, 1261–1274; b) J. Garcia-Amorós, M. C. R. Castro, P. Coelho, M. M. M. Raposo, D. Velasco, *Chem. Commun.* **2013**, *49*, 11427–11429; c) R. Travieso-Puente, S. Budzak, J. Chen, P. Stacko, J. T. Jastrzebski, D. Jacquemin, E. Otten, *J. Am. Chem. Soc.* **2017**, *139*, 3328–3331; d) C. E. Weston, R. D. Richardson, P. R. Haycock, A. J. White, M. J. Fuchter, *J. Am. Chem. Soc.* **2014**, *136*, 11878–11881; e) L. Stricker, M. Böckmann, T. M. Kirse, N. L. Doltsinis, B. J. Ravoo, *Chem. Eur. J.* **2018**, *24*, 8639–8647; f) A. D. W. Kennedy, I. Sandler, J. Andréasson, J. Ho, J. E. Beves, *Chem. Eur. J.* **2020**, *26*, 1103–1110.

[22] K. Mezgebe, E. Mulugeta, *RSC Adv.* **2022**, *12*, 25932–25946.

[23] S. R. Brishty, M. J. Hossain, M. U. Khandaker, M. R. I. Faruque, H. Osman, S. M. A. Rahman, *Front. Pharmacol.* **2021**, *12*, 762807.

[24] a) D. Dolles, A. Strasser, H.-J. Wittmann, O. Marinelli, M. Nabissi, R. G. Pertwee, M. Decker, *Adv. Ther.* **2018**, *1*, 1700032; b) S. Crespi, N. A. Simeth, A. Bellisario, M. Fagnoni, B. König, *J. Phys. Chem. A.* **2019**, *123*, 1814–1823; c) Y. Hasegawa, S. Kume, H. Nishihara, *Dalton Trans.* **2009**, 280–284; d) O. Shinzi, I. Syoji, M. Hiroshi, M. Mizuo, *Chem. Lett.* **2010**, *39*, 956–957.

[25] S. A. M. Steinmüller, J. Fender, M. H. Deventer, A. Tutov, K. Lorenz, C. P. Stove, J. N. Hislop, M. Decker, *Angew. Chem. Int. Ed. Engl.* **2023**, *62*, e202306176.

[26] R. Wong, S. J. Dolman, *J. Org. Chem.* **2007**, *72*, 3969–3971.

[27] A. A. John, Q. Lin, *J. Org. Chem.* **2017**, *82*, 9873–9876.

[28] a) F. Bureš, *RSC Adv.* **2014**, *4*, 58826–58851; b) C. Knie, M. Utecht, F. Zhao, H. Kulla, S. Kovalenko, A. M. Brouwer, P. Saalfrank, S. Hecht, D. Bléger, *Chem. Eur. J.* **2014**, *20*, 16492–16501; c) M. Dong, A. Babalhavaeji, S. Samanta, A. A. Beharry, G. A. Woolley, *Acc. Chem. Res.* **2015**, *48*, 2662–2670; d) J. Garcia-Amoros, D. Velasco, *Beilstein J. Org. Chem.* **2012**, *8*, 1003–1017.

[29] F. Riefolo, C. Matera, A. Garrido-Charles, A. M. J. Gomila, R. Sortino, L. Agnetta, E. Claro, R. Masgrau, U. Holzgrabe, M. Batlle, M. Decker, E. Guasch, P. Gorostiza, *J. Am. Chem. Soc.* **2019**, *141*, 7628–7636.

[30] N. A. Simeth, S. Crespi, M. Fagnoni, B. König, *J. Am. Chem. Soc.* **2018**, *140*, 2940–2946.

[31] a) L. Stricker, E.-C. Fritz, M. Peterlechner, N. L. Doltsinis, B. J. Ravoo, *J. Am. Chem. Soc.* **2016**, *138*, 4547–4554; b) M. A. Kienzler, A. Reiner, E. Trautman, S. Yoo, D. Trauner, E. Y. Isacoff, *J. Am. Chem. Soc.* **2013**, *135*, 17683–17686; c) A. A. Beharry, G. A. Woolley, *Chem. Soc. Rev.* **2011**, *40*, 4422–4437; d) C. Fedele, T.-P. Ruoko, K. Kuntze, M. Virkki, A. Priimagi, *Photochem. Photobiol. Sci.* **2022**, *21*, 1719–1734.

[32] a) E. A. Fink, J. Xu, H. Hübner, J. M. Braz, P. Seemann, C. Avet, V. Craik, D. Weikert, M. F. Schmidt, C. M. Webb, N. A. Tolmachova, Y. S. Moroz, X. P. Huang, C. Kalyanaraman, S. Gahbauer, G. Chen, Z. Liu, M. P. Jacobson, J. J. Irwin, M. Bouvier, Y. Du, B. K. Shoichet, A. I. Basbaum, P. Gmeiner, *Science* **2022**, *377*, eabn7065; b) J. Quoyer, J. M. Janz, J. Luo, Y. Ren, S. Armando, V. Lukashova, J. L. Benovic, K. E. Carlson, S. W. Hunt, M. Bouvier, *Proc. Natl. Acad. Sci. USA* **2013**, *110*, E5088–E5097; c) C. Galés, J. J. Van Durm, S. Schaak, S. Pontier, Y. Percherancier, M. Audet, H. Paris, M. Bouvier, *Nat. Struct. Mol. Biol.* **2006**, *13*, 778–786.

[33] a) H. Liu, J. Hofmann, I. Fish, B. Schaake, K. Eitel, A. Bartuschat, J. Kaindl, H. Rampp, A. Banerjee, H. Hübner, M. J. Clark, S. G. Vincent, J. T. Fisher, M. R. Heinrich, K. Hirata, X. Liu, R. K. Sunahara, B. K. Shoichet, B. K. Kobilka, P. Gmeiner, *Proc. Natl. Acad. Sci. USA* **2018**, *115*, 12046–12050; b) C. Gentzsch, K. Seier, A. Drakopoulos, M.-L. Jobin, Y. Lanoiselée, Z. Koszegi, D. Maurel, R. Sounier, H. Hübner, P. Gmeiner, S. Granier, D. Calebiro, M. Decker, *Angew. Chem. Int. Ed. Engl.* **2020**, *59*, 5958–5964.

[34] a) D. Weichert, A. C. Kruse, A. Manglik, C. Hiller, C. Zhang, H. Hübner, B. K. Kobilka, P. Gmeiner, *Proc. Natl. Acad. Sci. USA* **2014**, *111*, 10744–10748; b) R. C. Kling, M. Plomer, C. Lang, A. Banerjee, H. Hübner, P. Gmeiner, *ACS Chem. Biol.* **2016**, *11*, 869–875.

[35] a) H. Hübner, C. Haubmann, W. Utz, P. Gmeiner, *J. Med. Chem.* **2000**, *43*, 756–762; b) A. Drakopoulos, Z. Koszegi, Y. Lanoiselée, H. Hübner, P. Gmeiner, D. Calebiro, M. Decker, *J. Med. Chem.* **2020**, *63*, 3596–3609; c) O. H. Lowry, N. J. Rosebrough, A. L. Farr, R. J. Randall, *J. Biol. Chem.* **1951**, *193*, 265–275; d) Y. C. Cheng, W. H. Prusoff, *Biochem. Pharmacol.* **1973**, *22*, 3099–3108; e) G. M. Sheldrick, *Acta Crystallogr. Sect. A* **2015**, *71*, 3–8; f) O. V. Dolomanov, L. J. Bourhis, R. J. Gildea, J. A. K. Howard, H. Puschmann, *J. Appl. Crystallogr.* **2009**, *42*, 339–341; g) G. M. Sheldrick, *Acta Crystallogr. Sect. C* **2015**, *71*, 3–8.

Manuscript received: February 27, 2024
Accepted manuscript online: March 14, 2024
Version of record online: June 10, 2024